Anal. Chem. **2008,** *80,* 933−943

Covalent Virus Layer for Mass-Based Biosensing

Li-Mei C. Yang, Juan E. Diaz, Theresa M. McIntire, Gregory A. Weiss,* and Reginald M. Penner*

Department of Chemistry, University of California, Irvine, California 92697-2025

M13 virus particles were covalently attached to a planar gold-coated quartz crystal microbalance (QCM) through reaction with a self-assembled monolayer of *N*-hydroxysuccinimide thioctic ester, followed by incorporation of the blocking agent bovine serum albumin. This immobilization chemistry produced a phage multilayer having a coverage equivalent to ≈6.5 close-packed monolayers of the virus. The properties of this "covalent virus surface" or CVS for the mass-based detection of a 148.2 kDa antibody were then evaluated in a phosphate buffer using a flow injection analysis system. The mass of the CVS increased with exposure to an antibody (p-Ab) known to bind the phage particles with high affinity. Bound p-Ab was removed by washing with 0.5 M HCl thereby regenerating the sensor surface. A calibration plot for p-Ab binding was constructed by repetitively exposing the surface to p-Ab at concentrations between 6.6 and 200 nM and HCl rinsing after each exposure. The mass−concentration relationship was linear with a sensitivity of 0.018 μg/(cm^2 nM) and a limit of detection of 7 nM or 1.3 pmol. The CVS could be saturated with high doses of p-Ab enabling the determination that an average of ≈140 binding sites are available per M13 phage particle. Exposure of the CVS to a second, nonbinding antibody (n-Ab) did not cause a measurable mass change. These results demonstrate that the covalent virus layer is a rugged, selective, and sensitive means for carrying out mass-based biodetection.

Phage display can be used to prepare combinatorial protein libraries with up to 10^{11} unique members.[1−3] The tremendous sequence variability present in these libraries makes possible the identification of polypeptides that bind with high affinity (K_D < 10^{-8} M) to virtually any target molecule.[4] Secondary screens and selections against potentially interfering molecules can also tailor the specificity of selectants. Although typically only a limited number of selectants emerge from this intensive in vitro evolution, large quantities of each selectant can be rapidly produced through amplification in an *E. coli* host. This display "machinery" is ideally suited to the production of artificial receptors competitive with antibodies in terms of the strength and specificity of the molecular recognition interaction, but which can be produced in quantity easily and rapidly.[4,5] In addition, the phage display format allows rapid tailoring of binding properties, such as the use of homolog shotgun scanning for affinity maturation.[6,7]

A polypeptide selected from phage display can be resynthesized or expressed with an appropriate linker and used as a receptor in a biosensor (see, for example, refs 8 and 9). However, retaining the phage as a display scaffold offers important advantages. First, due to multicopy display on the surface of the phage, peptide selectants can exhibit enhanced affinities due to an avidity or "velcro" effect when attached to the phage; removal from the phage surface can dramatically decrease receptor affinity (for example, ref 6). Second, the filamentous phage particle can serve as a "carrier" for the selected receptor—a chemical recognition "module" that obviates additional steps required for synthesis of the free peptide, attachment of a linker, and finally conjugation of the receptor to the biosensor. Phage display can thus reduce the receptor immobilization challenge to a single phage bioconjugation step that is generalizable to every phage-displayed receptor.

In pursuit of this goal, we have been developing a modular biosensing platform in which peptides on the surface of the M13 bacteriophage perform the recognition and binding functions.[10] M13 virus particles are covalently attached to a self-assembled monolayer (SAM)[11] covalently bonded to a gold surface (Figure 1) to form a "covalent virus surface" ("CVS"). Also present in the CVS are molecules of bovine serum albumin (BSA) intended to fill residual pin-holes in the SAM and block the surface from nonspecific adsorption. In a preliminary examination of this biosensor,[10] we explored two modes of transduction: electrochemical impedance and mass (using a quartz crystal microbalance (QCM)). In this article, we report an in-depth examination of the properties of immobilized M13 and the CVS for the mass-based detection (Figure 2) of a 148.2 kDa antibody with binding specificity for the virus. From a quantitation perspective, this system represents a best-case scenario in which the antibody recognizes the P8 coat peptide that is expressed at a level of ≈2700 copies per phage particle. Peptides and proteins fused to P8 or

* To whom correspondence should be addressed. E-mail: gweiss@uci.edu (G.A.W.); rmpenner@uci.edu (R.M.P.).

(1) Scholle, M. D.; Kehoe, J. W.; Kay, B. K. *Comb. Chem. High Throughput Screening* **2005**, *8*, 545−551.
(2) Sidhu, S. S.; Fairbrother, W. J.; Deshayes, K. *ChemBioChem* **2003**, *4*, 14−25.
(3) Sidhu, S. S.; Weiss, G. A.; Wells, J. A. *J. Mol. Biol.* **2000**, *296*, 487−495.
(4) Smith, G. P.; Petrenko, V. A. *Chem. Rev.* **1997**, *97*, 391−410.
(5) Kehoe, J. W.; Kay, B. K. *Chem. Rev.* **2005**, *105*, 4056−4072.
(6) Murase, K.; Morrison, K. L.; Tam, P. Y.; Stafford, R. L.; Jurnak, F.; Weiss, G. A. *Chem. Biol.* **2003**, *10*, 161−168.
(7) Sato, K.; Simon, M. D.; Levin, A. M.; Shokat, K. M.; Weiss, G. A. *Chem. Biol.* **2004**, *11*, 1017−1023.
(8) Goldman, E. R.; Pazirandeh, M. P.; Charles, P. T.; Balighian, E. D.; Anderson, G. P. *Anal. Chim. Acta* **2002**, *457*, 13−19.
(9) Goldman, E. R.; Pazirandeh, M. P.; Mauro, J. M.; King, K. D.; Frey, J. C.; Anderson, G. P. *J. Mol. Recognit.* **2000**, *13*, 382−387.
(10) Yang, L. M. C.; Tam, P. Y.; Murray, B. J.; McIntire, T. M.; Overstreet, C. M.; Weiss, G. A.; Penner, R. M. *Anal. Chem.* **2006**, *78*, 3265−3270.
(11) Cheng, Q.; Brajter-Toth, A. *Anal. Chem.* **1992**, *64*, 1998−2000.

10.1021/ac071470f CCC: $40.75
Published on Web 01/17/2008

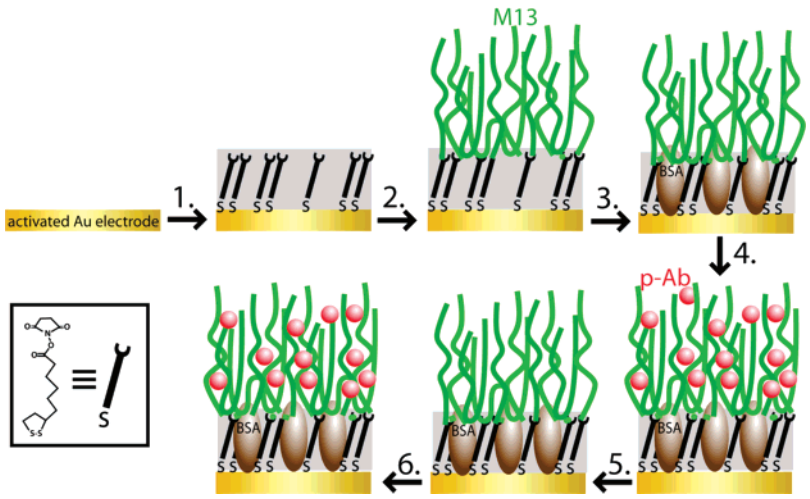

Figure 1. Schematic diagram depicting the stepwise assembly (steps 1−3) and functionalization (steps 4−6) of the covalent virus surface, CVS, evaluated in this study.

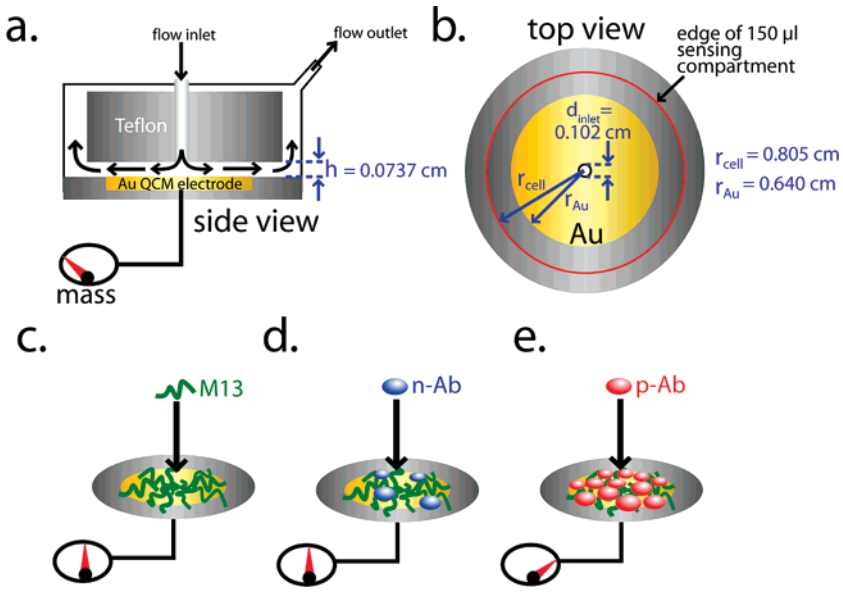

Figure 2. Schematic diagram (not to scale) of the flow cell and the sensing scheme explored in this study. (a) Side view of the stagnation point flow cell for QCM measurements. (b) Top view of this cell, showing the QCM radius and the flow cell radius. The volume of the sensing compartment was 150 μL. (c−e) Schematically, we show here the rejection of nonspecific binding of the negative antibody (n-Ab) and the selective binding of the antibody (p-Ab) specific for the P8 principle coat peptide of M13.

P3 are typically displayed at much lower levels, ranging from a hundred displayed per phage to less than one copy of displayed receptor per phage. In addition, the affinity between the displayed receptor and target protein can vary from very high binding affinities that slightly exceed the antibody−P8 interaction reported here[12] to much lower affinities.[6]

We are not the first to explore the use of whole phage in biosensors: Anderson and co-workers[8,9] employed fluorescently labeled phage particles as reagents in detectors for *staphylococcal enterotoxin B* and 2,4,6 trinitrotoluene (TNT). In 2003 Petrenko and Vodyanoy [13] tethered biotinylated M13 phage to a biotinylated Langmuir−Blodgett layer on a gold-coated acoustic wave sensor via a steptavidin linker. Vodyanoy's group[14] have evaluated a simpler immobilization strategy involving the direct physisorption of phage particles onto gold-coated acoustic wave mass sensors or QCMs.[14,15] This research group also employed surface plasmon resonance (SPR) spectroscopy as a means for detecting the binding of β-galactosidase, also using physisorbed phage layers.[16]

Virus particles have also been immobilized on sensor surfaces for the purpose of measuring their concentration in solution. Klenerman and co-workers[17,18] immobilized phage particles, including M13,[18] on gold-coated QCM electrodes and then measured the detachment of these particles induced by the sheer

(12) Dennis, M. S.; Eigenbrot, C.; Skelton, N. J.; Ultsch, M. H.; Santell, L.; Dwyer, M. A.; O'Connell, M. P.; Lazarus, R. A. *Nature* **2000**, *404*, 465−470.
(13) Petrenko, V. A.; Vodyanoy, V. J. *J. Microbiol. Methods* **2003**, *53*, 253−262.
(14) Nanduri, V.; Sorokulova, I. B.; Samoylov, A. M.; Simonian, A. L.; Petrenko, V. A.; Vodyanoy, V. *Biosens. Bioelectron.* **2007**, *22*, 986−992.
(15) Olsen, E. V.; Sorokulova, I. B.; Petrenko, V. A.; Chen, I. H.; Barbaree, J. M.; Vodyanoy, V. J. *Biosens. Bioelectron.* **2006**, *21*, 1434−1442.
(16) Nanduri, V.; Balasubramanian, S.; Sista, S.; Vodyanoy, V. J.; Simonian, A. L. *Anal. Chim. Acta* **2007**, *589*, 166−172.
(17) Cooper, M. A.; Dultsev, F. N.; Minson, T.; Ostanin, V. P.; Abell, C.; Klenerman, D. *Nat. Biotechnol.* **2001**, *19*, 833−837.
(18) Dultsev, F. N.; Speight, R. E.; Florini, M. T.; Blackburn, J. M.; Abell, C.; Ostanin, V. P.; Klenerman, D. *Anal. Chem.* **2001**, *73*, 3935−3939.

forces imparted by the QCM itself. The means of phage attachment in this case was a SAM of a mercapto-undecanoic acid conjugated to a monoclonal antibody for the virus.

EXPERIMENTAL SECTION

Materials. All chemicals and solvents (>99% purity) were purchased from Fisher or Merck and used as received, unless noted. Dimethylformamide (DMF) and ethanol were dried with 4 Å molecular sieves obtained from Alfa. The anti-M13 antibody (p-Ab) was purchased from GE Healthcare, and the anti-Flag M2 (n-Ab) was purchased from Sigma. Millipore-filtered water (resistance ≈18 MΩ cm) was used in all experiments. Phosphate-buffered fluoride buffer, PBF (4.2 mM Na_2HPO_4, 1.5 mM KH_2PO_4, 140 mM NaF, pH 7.2), was filter-sterilized through a 0.22 μm pore size membrane (Corning). The wash buffer was 0.06% BSA, 0.07% Tween 20 (Sigma) in PBF buffer. BSA (0.2%) in phosphate-buffered sodium fluoride (pH 7.2) solution was used for blocking (all percentages provided as w/v). Various concentrations of acid wash solutions were prepared from 2 M HCl diluted with water and mixed with 0.1% Tween 20.

Phage Enzyme-Linked Immunosorbent Assay for Determining KO7−p-Ab Apparent Binding Affinity. A Maxisorp immunoplate (96-well) was coated with M13 KO7 phage for 1 h at room temperature (100 μL, 10 nM in 50 mM sodium carbonate buffer, pH 9.6). The plate was then blocked for 30 min at room temperature with BSA (0.2%) in PBS and washed five times with PT buffer (PBS, 0.05% Tween 20). The coated wells were incubated with anti-M13 monoclonal antibody (100 μL) at concentrations ranging from 5 nM to 2 pM in PBS, BSA (0.1%), Tween 20 (0.1%) for 1 h at room temperature and washed five times with PT buffer. After washing, the plate was incubated with antimouse IgG/horseradish peroxidase conjugate (100 μL, 1:2000) in PBS, BSA (0.1%), Tween 20 (0.1%) for 1 h, then washed five times with PT and twice with PBS. The plate was developed by using an *o*-phenylenediamine dihydrochloride/H_2O_2 solution (100 μL, 1 mg mL^{-1}/0.02%) and read spectrophotometrically at 450 nm.

Virus Immobilization and QCM Measurements. The details of our method for virus immobilization are described in detail in ref 10. QCM measurements were carried out using gold-coated AT-cut oscillator electrodes (Stanford Research Systems) on which the virus immobilization chemistry, described above, had been carried out. The frequency of this crystal as well as its motional resistance were measured using a Stanford Research Systems frequency digital controller (model QCM 200) and 5 MHz crystal oscillator (model QCM 25) interfaced to a computer. QCM gravimetry was calibrated by comparing the charge associated with the electrodeposition of silver onto the QCM crystal with the observed frequency change. Silver electrodeposition was carried out from aqueous ≈10 mM AgF in 0.10 M NaF, and a Coulombic efficiency of unity was assumed. The QCM crystal was mounted in a Teflon flow cell (Stanford Research Systems) that provided for the radially symmetric delivery (stagnation point geometry[19]) of solution to the circular QCM electrode surface, as shown in Figure 2. The total volume of this flow cell, measured between the inlet and the exit port, was 1150 μL, but the volume of the QCM crystal chamber was 150 μL. This flow cell was supplied via a flow injection analysis system that contained the following components: a syringe pump (Kd Scientific Inc., KDS101), flexible Teflon tubing (o.d. $^1/_{16}$ in., Dupont), and a six-port HPLC medium pressure injection rotary valve (Western Analytical Products) fitted with a Teflon 180 μL sample loop. In addition to providing for the delivery of the p-Ab and n-Ab analytes, this injection system was employed for the rinse solutions (like wash buffer), including 0.5 M HCl, described below.

A sample volume of 180 μL and a volumetric flow rate of 30 μL/min were used for most of the measurements reported below. In conjunction with the 150 μL crystal chamber volume, the contact time of the sample bolus with the QCM was 660 s (= 180 μL/(30 μL/min) + 150 μL/(30 μL/min)).

Atomic Force Microscopy Analysis. Intermittent contact mode atomic force microscopy (AFM) imaging was performed in air at ambient pressure and humidity using an AutoProbe CP-Research (ThermoMicroscopes, Sunnyvale, CA; now Veeco Instruments, Santa Barbara, CA) scanning probe microscope. The piezoelectric scanner was calibrated using a 5.0 μm grating in the *xy* and *z* directions using an AFM reference (Pacific Nanotechnology, Santa Clara, CA; model no. P-000-0004-0). The AFM tips were silicon (either Multi75 Metrology Probes, model no. MPP-21100; or Tap300 Metrology Probes, model no. MPP-11200, both Veeco Instruments, Santa Barbara, CA). Topographs were obtained as 256 × 256 pixels, flattened line by line, and analyzed using the AutoProbe image processing software supplied by the manufacturer of the AFM. The root-mean-square (rms) surface roughness over selected scanned areas was calculated from the formula $R_{rms} = [\sum^N (z_n - \bar{z})^2/(N-1)]^{1/2}$, where $\bar{z}$ is the average *z* height, z_n is the height at each point on the sample, and N is the number of points sampled.

RESULTS AND DISCUSSION

M13, a filamentous *E. coli* bacteriophage, is commonly used for phage display because it replicates without destroying the host bacterium.[4] The M13 virion is 1−2 μm in length and 6 nm in diameter (see the AFM image in Figure 3a). The lateral surfaces of the M13 virion are covered with ≈2700 copies of P8, the major coat protein having 50 residues. The ends of the capsid are capped with five copies each of the minor coat proteins, either P3/P6 or P7/P9. In an AFM image (Figure 3a), the P3/P6 end of the virion can be readily distinguished due to the greater diameter associated with the larger size of these minor coat proteins. Each P8 can bind to the antibody employed in this investigation. As measured by enzyme-linked immunosorbent assay (ELISA), the anti-M13 antibody binds to the virus with an EC_{50} or apparent K_D of 200 pM (Supporting Information Figure S1). This antibody, which we shall refer to as "p-Ab", has a molecular mass of 148.2 ± 0.3 kDa as measured by time-of-flight mass spectrometry (Supporting Information Figure S2).

M13 virions attached to a gold surface using the scheme outlined in Figure 1 form an interpenetrating random network on the *N*-hydroxysuccinimide thioctic ester (NHS-TE) SAM layer that can be visualized by AFM. Typical AFM images of a polycrystalline gold surface on which the NHS-TE SAM has been prepared and a similar surface that was also reacted with M13 are shown in Figure 3, parts b and c, respectively. On the M13-reacted surface (Figure 3c), two features are observed that are not seen on the control surface of Figure 3b: long strings with

(19) van Duijvenbode, R. C.; Koper, G. J. M. *J. Phys. Chem. B* **2001**, *105*, 11729−11736.

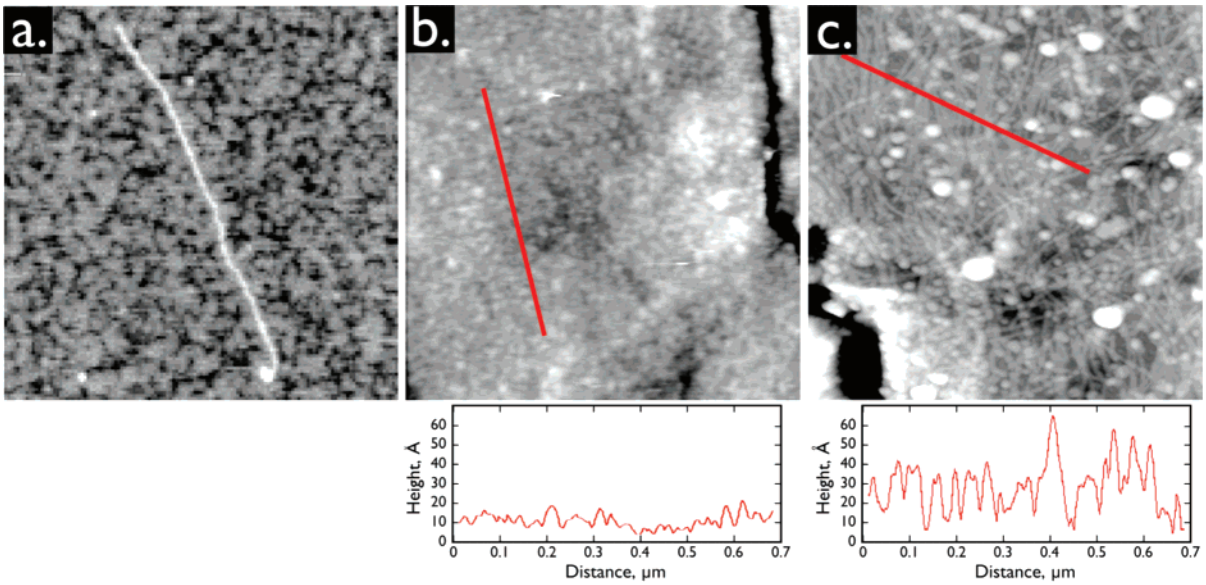

Figure 3. Noncontact mode atomic force microscope (AFM) images (1 μm × 1 μm) acquired in air. (a) A single M13 virion on mica prepared by spraying from a virus suspension. The mottled gray background is typical of a partially hydrated mica surface. (b) A self-assembled monolayer (SAM) of *N*-hydroxysuccinimide thioctic ester on polycrystalline gold after exposure to BSA. No virions were attached to this surface. The dark fissure at upper right is a grain boundary. (c) A functional covalent virus layer consisting of a SAM of *N*-hydroxysuccinimide thioctic ester (NHS-TE) on polycrystalline gold, reacted first with M13 to produce covalent attachment, and then exposed to BSA (Figure 1, step 3). The dark fissure at lower left is a grain boundary.

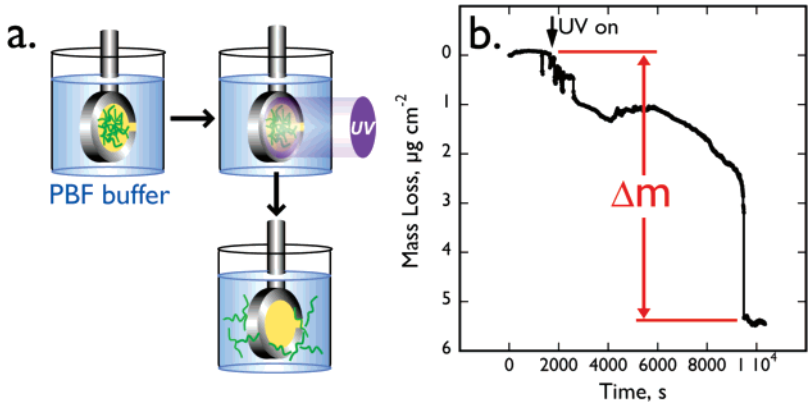

Figure 4. QCM measurement of the detachment of the SAM and phage layer induced by UV photolysis. (a) Schematic description of the phage- and SAM-modified QCM electrode immersed in a 250 mL beaker with PBF buffer solution and illuminated by 365 nm UV light at 18 mW for 2.5 h. (b) Mass vs time during the UV exposure. An abrupt mass loss, such as seen here at 9500 s, was characteristic of this process. The total mass of attached M13 phage was taken to be the measured ΔM minus a mass of 1.5 μg/cm^2, associated with the weak, noncovalent binding of phage to the sensor surface.

heights ranging from 10 to 30 nm and globular particles with a height of 100−200 nm. We believe both structures derive from M13 virions and aggregates of several viral filaments. The globular P3s from multiple M13 virions could also aggregate to produce some of the larger spheroids seen in these images. However, we cannot rule out the possibility that some spheroids are produced by coiled phage filaments.

The AFM shows the topography of the CVS, but the images do not reveal the total number of virus particles bound to the surface. The total amount of M13 present on this surface can be estimated by recording the mass loss from the surface as the phage and SAM layer are removed. We note here that this estimate—and all other metrics derived from mass changes measured for this system—will be approximate[20] because the CVS under investigation here is not rigidly coupled to the QCM surface. We discuss the dissipation of energy by the CVS below.

Phage were detached from the gold surface by photooxidizing the thiol SAM using UV light,[21] as shown schematically in Figure 4a. Mass loss from a CVS immersed in PBF buffer commences promptly with UV light illumination, and the ensuing mass loss transient (Figure 4b) is always characterized by a sharp drop in mass after which the mass stabilizes at a new value. Assuming the entire mass loss is associated with phage (the mass of the NHS-TE monolayer is negligible), the total phage coverage measured in this way was 3.0 μg cm^{-2} corresponding to 1.1 × 10^{11} particles cm^{-2} or the equivalent of 6.5 close-packed monolayers. This density represents a capture efficiency of approximately 10% of the phage available during surface attachment. Still, the phage loading reported here is 70% higher than the highest loading achieved by Vodyanoy and co-workers[14,15] who evaluated

(20) Buttry, D. A.; Ward, M. D. *Chem. Rev.* **1992**, *92*, 1355−1379.
(21) Huang, J. Y.; Hemminger, J. C. *J. Am. Chem. Soc.* **1993**, *115*, 3342−3343.

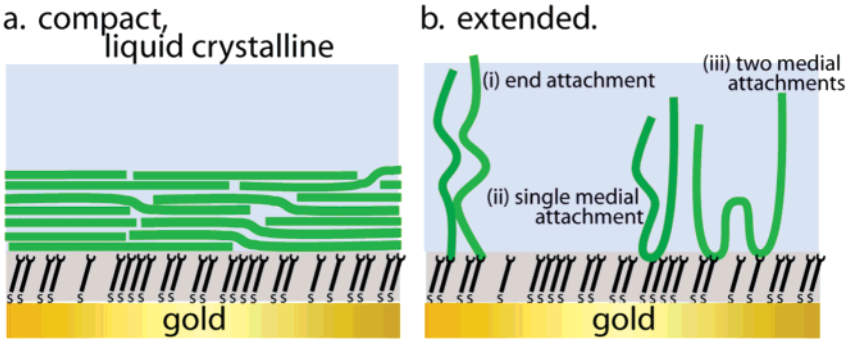

Figure 5. Schematic depiction of two limiting structures for the organization of phage multilayers: (a) compact, liquid crystalline; (b) extended, three-dimensional. In this rendering, just four virus particles are depicted for purposes of clarity.

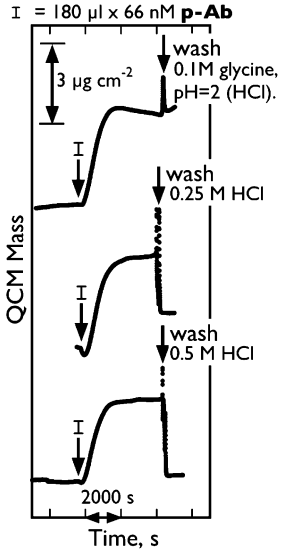

Figure 6. QCM evaluation of the efficacy of three wash solutions: (top) 0.1 M glycine (pH ~ 2 adjusted with HCl), (middle) 0.25 M HCl, and (bottom) 0.5 M HCl. In all three cases, a CVS was exposed to 180 μL of 66 nM p-Ab in wash buffer at 30 μL min^{-1}. The wash was carried out at a higher flow rate of 100 μL min^{-1}.

direct phage physisorption of M13 onto a bare gold surface as a means for immobilization.

The presence of multiple monolayers of phage suggests that the CVS is a three-dimensional network of M13 filaments with a minimum of 6−7 viral diameters or ≈40 nm in total thickness. This multilayer structure cannot be achieved by layering phage in a liquid crystalline arrangement parallel to the QCM surface (Figure 5a), because contact and covalent bonding can only occur between the gold surface and the first closest-packed phage layer. In this parallel configuration, phage layers above the first covalently tethered layer would be desorbed rapidly into the mobile phase, and this is not observed. Instead, we expect that each phage particle is anchored by one or more amide bond attachment points to the SAM and that unbound segments of the virus filaments are free to extend from these attachment points away from the SAM monolayer, as shown schematically in Figure 5b. Importantly, the two structures shown in Figure 5 can appear indistinguishable in AFM images of this surface acquired in air (e.g., Figure 3c) since the extended structure seen in Figure 5b can be expected to collapse onto the surface in the absence of the buffer solution.

The mass responses of a CVS to injections of 180 μL of 66 nM p-Ab (≈12 pmol) are shown in Figure 6. The mass of the surface increased over the course of the exposure and stabilized at a new mass that was larger by 3−4 μg cm^{-2}. This loading of p-Ab was retained by the surface over a period of hours (data not shown) with negligible loss. The efficacy of several wash solutions is shown in Figure 6: acidic (pH = 2.0), 0.1 M glycine had virtually no effect on the binding of p-Ab to the surface, but 0.25 M HCl consistently removed 60−80% of the bound p-Ab over the course of a minute or less, and the slightly higher concentration of 0.5 M HCl quantitatively removed bound p-Ab over the same period, restoring the sensor mass to ±2% of its value prior to p-Ab exposure. On the basis of these results, 0.5 M HCl became the standard wash solution used for the construction of calibration curves for the QCM response to various concentrations of p-Ab (vide infra).

In these experiments, we are operating in a regime of flow rate in which the rate of antibody attachment to the CVS shows an unusually strong sensitivity to the volumetric flow rate, u. At flow rates of 50 μL min^{-1} or higher, no QCM response at all was observed (Figure 7a). As the flow rate was reduced from 50 μL min^{-1}, the mass sensitivity increased rapidly and quasi-linearly (Figure 7b). In fact, the effect of flow rate on antibody binding is stronger than expected for pure diffusion-controlled binding of the antibody to the CVS based on the following analysis: It is well-established that the flux of molecules at a planar biosensor surface increases in proportion to $u^{1/3}$.[22,23] For a series of injections of constant volume, the time of exposure of the surface to the analyte solution will be proportional to u^{-1}, and we therefore conclude that the diffusion-controlled mass loading should increase in proportion to $(u^{-1})(u^{1/3}) = u^{-2/3}$ as previously observed,[23] whereas the best fit of a power series in u to these data is obtained with $u^{-1.94}$ (Figure 7b).

We do not have sufficient data to explain this unusual u dependence; however, one possible explanation is that the three-dimensional phage layer undergoes shear flow-induced morphological changes that reduces the affinity of the CVS for p-Ab at higher flow rates. Because of the stagnation point geometry of our flow cell (Figure 2, parts a and b), the wall shear rate, γ, is inversely proportional to the radius measured from the stagnation point, r_{cell}, according to[24]

$$\gamma = \frac{3u}{\pi r_{cell} h^2} \quad (1)$$

(22) Matsuda, H. *J. Electroanal. Chem.* **1967**, *15*, 325 ff.

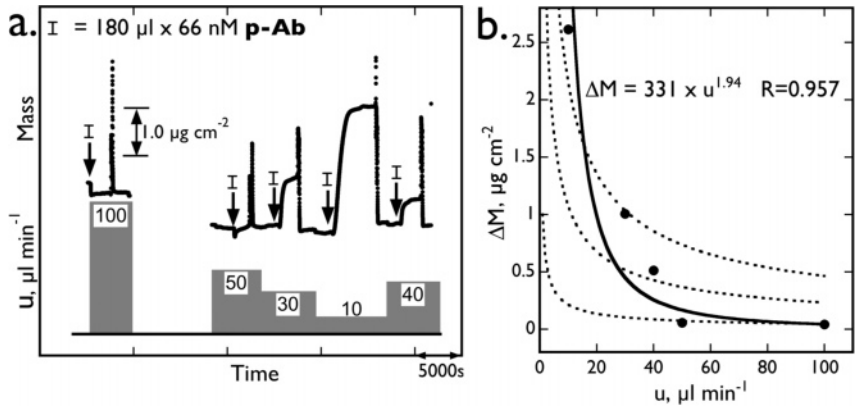

Figure 7. Effect of flow rate, u, on the measured mass transient induced by exposure to 180 μL of 66 nM p-Ab. (a) The mass vs time for five flow rates (bottom) varying from 10 to 100 μL min^{-1}. Arrows indicate injection times. Bound p-Ab was removed by washing with 180 μL of 0.5 M HCl after each injection. (b) Plot of ΔM increase vs u for the data shown in (a). The solid line is the best fit of a power series in u to these data. Dashed lines show three $u^{-2/3}$ proportional fits to these data.

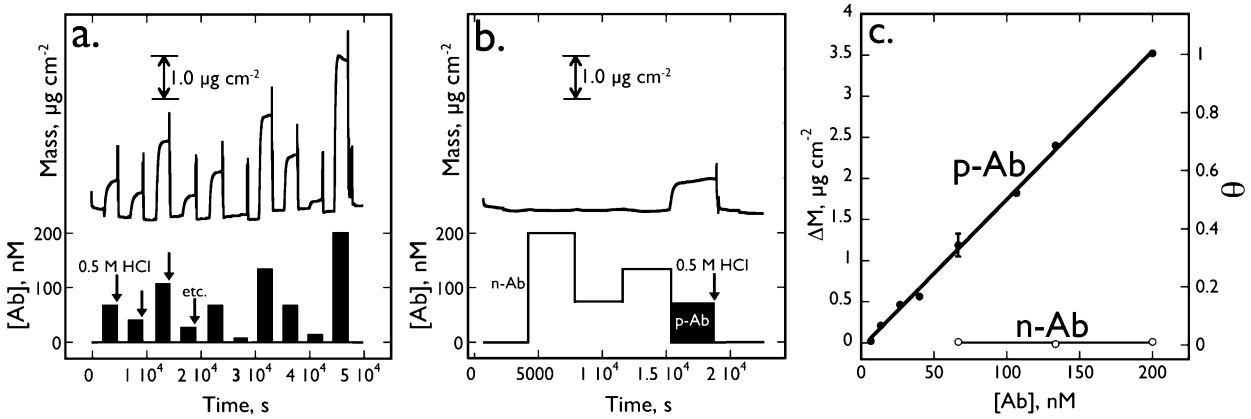

Figure 8. Construction and analysis of the p-Ab calibration plot. (a) Plot of mass vs time (top) for the exposure of a CVS to 10 180 μL doses of p-Ab, ranging in concentration from 6.6 to 200 nM (black bars, bottom). Flow rate = 30 μL min^{-1}. Note that exposure of the CVS to p-Ab occurs only during the first ≈360 s. Bound p-Ab was removed after each injection using 180 μL of 0.5 M HCl (arrows). (b) Effect of exposure to n-Ab on the response of a CVS. In this experiment, three 180 μL injections of n-Ab were sequentially administered at concentrations of 200, 66, and 120 nM (white bars, bottom). Then a single 180 μL injection of 66 nM p-Ab (black bar, bottom) was administered. (c) Plot of maximum mass change vs p-Ab concentration for the data shown in (a). The mass change was proportional to the concentrations of injected p-Ab (R^2 = 0.997) and yielded a sensitivity of 0.018 μg cm^{-2}/nM and a limit of detection (LOD) of 6.6 nM.

where h is the chamber height. The applicable range of γ values is obtained by calculating the highest γ at the edge of the inlet port (r_{cell} = 0.051 cm) and the lowest γ at the perimeter of the gold QCM electrode (r_{cell} = 0.640 cm). The γ ranges ($\gamma_{high}-\gamma_{low}$) so calculated are as follows: u = 30 μL/min (0.137−1.73 s^{-1}), u = 50 μL/min (0.228−2.88 s^{-1}), and u = 100 μL/min (0.456−5.77 s^{-1}). These values are not extraordinary, being within the range of wall shear rates typically obtained for QCM measurements conducted in flow cells similar to the one employed here, cf., refs 25−28. So although the flow rate dependence we see in Figure 7 is unusual, the wall shear rate generated over this range of flow rates is not unusual. For all subsequent measurements discussed below, a flow rate of 30 μL min^{-1}, which is in the middle of the quasi-linear region seen in Figure 7b, was used.

A calibration plot for the binding of p-Ab to the CVS was constructed by recording the mass increases associated with exposure of the surface to injections of p-Ab at concentrations varying from 6.6 to 200 nM (Figure 8a). After each 180 μL injection, approximately 2400 s was allowed to elapse after which the bound p-Ab was removed by washing with 180 μL of 0.5 M HCl thereby regenerating the CVS. Each mass transient seen in Figure 8a shows the same pattern: After each injection in the data set of Figure 8a, the mass of the CVS increased for an average of 760 ± 350 s and then stabilized at a value proportional to the concentration of p-Ab (Figure 8c). As indicated by its standard deviation of 350 s, this "rise-time" (to 90% maximum mass) was subject to considerable experimental uncertainty, but the mean value approximates the calculated 660 s contact time of the p-Ab bolus with the CVS-modified gold QCM electrode. The CVS was then regenerated after ≈2400 s by injecting 180 μL of 0.5 M HCl using a higher flow rate of 100 μL min^{-1}. We also investigated

(23) Sjolander, S.; Urbaniczky, C. *Anal. Chem.* **1991**, *63*, 2338−2345.
(24) Truskey, G. A.; Yuan, F.; Katz, D. F. *Transport Phenomena in Biological Systems*; Pearson Prentice Hall: Upper Saddle River, NJ, 2004.
(25) Christ, K.; Wiedemann, I.; Bakowsky, U.; Sahl, H. G.; Bendas, G. *Biochim. Biophys. Acta* **2007**, *1768*, 694−704.
(26) Hook, F.; Voros, J.; Rodahl, M.; Kurrat, R.; Boni, P.; Ramsden, J. J.; Textor, M.; Spencer, N. D.; Tengvall, P.; Gold, J.; Kasemo, B. *Colloids Surf., B* **2002**, *24*, 155−170.
(27) Pierres, A.; Tissot, O.; Malissen, B.; Bongrand, P. *J. Cell Biol.* **1994**, *125*, 945−953.
(28) Sin, A.; Murthy, S. K.; Revzin, A.; Tompkins, R. G.; Toner, M. *Biotechnol. Bioeng.* **2005**, *91*, 816−826.

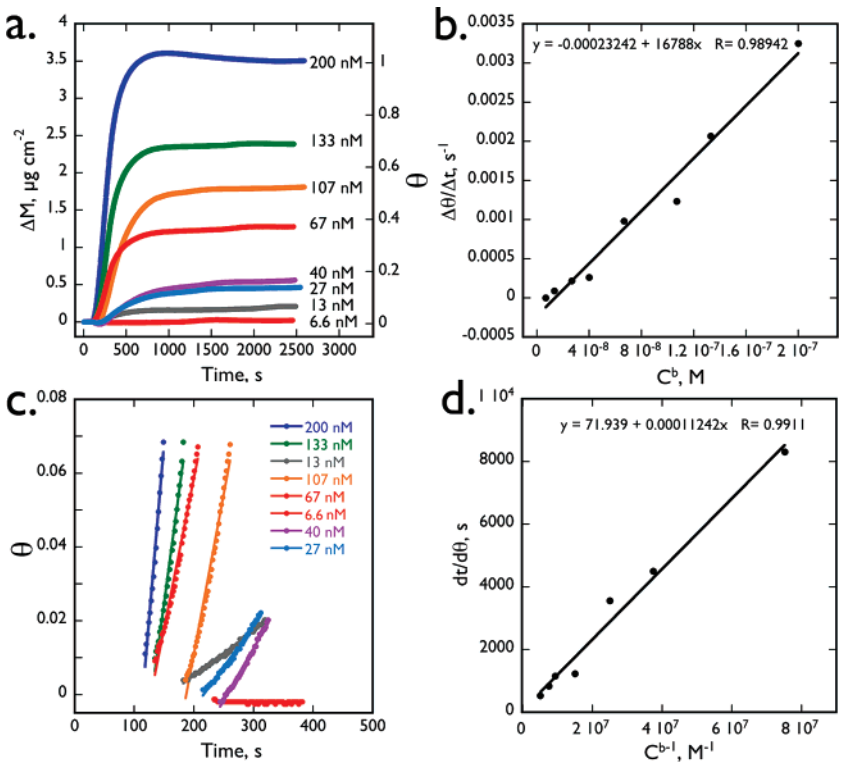

Figure 9. Determination of k_a: (a) Plot of frequency vs time acquired during the experiment of Figure 8 normalized to the same starting time and mass. (b) Plot of $\Delta\theta/\Delta t$ for the data shown in (a) evaluated in the region $0.2 < \theta/\theta_{max} < 0.8$ where θ_{max} is the value of θ seen at the plateau for each value of C^b. The slope of this plot provides an estimate of the quantity $D/\delta\Gamma^S = 1.7 \times 10^7$ cm^3 mol^{-1} s^{-1}. (c) Expansion of the low-mass region of the transients shown in (a). The least-squares fit to the QCM data are shown as solid lines in this plot, and the experimental data are shown as points. (d) Plot of $(d\theta/dt)^{-1}$ obtained from (c) vs $1/C^b$ for the seven trials analyzed in (a). In conjunction with the value of $D/\delta\Gamma^S$, the slope of this plot yields a k_a value of $(1.9 \pm 0.1) \times 10^4$ M^{-1} s^{-1}.

the response of the CVS to a control antibody, n-Ab, which showed no measurable affinity for K07 phage in ELISA binding measurements (ELISA with n-Ab data not shown). The CVS showed no measurable mass increase upon exposures to n-Ab at concentrations up to 200 nM (Figure 8b).

The limit of detection (LOD) for p-Ab demonstrated in Figure 8a is 6.6 nM. A lower LOD should be attainable since the QCM noise floor, measured from the rms of a PBF buffer blank, corresponded to a p-Ab concentration of just 0.3 nM. A lower LOD in the 1 nM range is also expected based upon the upper limit for K_D which we estimate (see below) to be 0.5 nM and with the apparent K_D of 0.2 nM measured by ELISA (Supporting Information Figure S1). Since the experiment of Figure 8a requires the CVS to endure nearly 14 h of continuous exposure to flowing PBF wash buffer, the linearity of the calibration curve derived from this experiment is testimony both to the remarkable stability of the CVS surface and to the reproducibility of its affinity for p-Ab. The mass drift seen in the baseline over this period was ± 0.2 μg cm^{-2}.

The linear calibration curve of Figure 8c is unusual, especially when it is considered that the fraction of available binding sites occupied by p-Ab, θ, varies from 0.03 to 1.0 (Figure 8c) over this concentration range. Note that saturation, corresponding to $\theta = 1.0$, is just achieved with the injection of 200 nM, as evidenced by the release of unbound, excess p-Ab from the surface following this injection as seen most clearly in Figure 9a. The linearity of this calibration curve is consistent with the diffusion-controlled binding of p-Ab to the CVS over this entire range of p-Ab concentrations from 6.6 to 200 nM. The following discussion applies the theoretical treatment and formalism of Bourdillon et al.[29] to the analysis of the binding of p-Ab to the P8 epitopes (ϕ) of the immobilized M13.[29] The reaction of interest is:

$$\phi + \text{p-Ab} \underset{k_d}{\overset{k_a}{\rightleftharpoons}} \phi\text{p-Ab} \qquad (2)$$

where k_a and k_d are, respectively, the rate constants for association and dissociation of p-Ab with ϕ. Their analysis included mass transport and assumed a Langmuir isotherm for p-Ab adsorption. The following differential equation was derived for the time rate of change of the fraction of available ϕ sites occupied by p-Ab, θ:[29]

$$\frac{d\theta}{dt} = \frac{k_a C^b (1-\theta) - k_d \theta}{1 + k_a C^b t_d (1-\theta)} \qquad (3)$$

where the total surface concentration of immobilized receptor, $\Gamma^S = \Gamma_\phi + \Gamma_{\phi p-Ab}$, $\theta = \Gamma_{\phi p-Ab}/\Gamma^S$, C^b is the bulk concentration of p-Ab in the solution, and t_d is a time characterizing the diffusional transport of p-Ab to the sensor surface:

(29) Bourdillon, C.; Demaille, C.; Moiroux, J.; Saveant, J. M. *J. Am. Chem. Soc.* **1999**, *121*, 2401−2408.

$$t_d = \frac{\delta\Gamma^S}{DC^b} \quad (4)$$

where δ is the steady-state thickness of the diffusion/convection layer and D is the diffusion coefficient for p-Ab.[29]

Bourdillon et al. showed that the integrated solution of eq 3 adopts a particularly simple, limiting form when $K = k_a/k_d$ is large and diffusion is rate-limiting:[29]

$$\theta = \frac{\theta_{eq} t D C^b}{\delta\Gamma^S} \quad (5)$$

where θ_{eq} is the equilibrium coverage of the CVS by p-Ab at a concentration C^b. t in eq 5 is the total time during which the solution of p-Ab is in contact with the CVS. For the flow cell shown in Figure 2, parts a and b, t is the injected volume divided by the flow rate: $t = 180\ \mu L/(30\ \mu L\ min^{-1}) = 6.0\ min = 360\ s$. Equation 5 predicts a linear calibration curve (i.e., θ vs C^b) if $\theta_{eq} = 1.0$ over the entire concentration range which, as we shall show, is the case here. The slope of the linear calibration curve in Figure 8c can be used to determine the value of a collection of constants, $D/\delta\Gamma^S$, that characterize the diffusive transport of p-Ab to the CVS: $D/\delta\Gamma^S = 1.4 \times 10^7\ cm^3\ mol^{-1}\ s^{-1}$.

This result provides a means for estimating k_a. This estimate is obtained by measuring the binding rate in the limit of low p-Ab coverage. For $\theta \ll 1$, eq 3 simplifies to

$$\frac{d\theta}{dt} = \frac{k_a C^b}{1 + k_a C^b t_d} \quad (6)$$

The differential quantity on the left-hand side of eq 6 can be directly evaluated from the mass versus time response data of Figure 8a and replotted in Figure 9c at very low θ values, below 0.05. With the use of $d\theta/dt$ values in this range, the reciprocal of eq 6 permits an estimated k_a to be obtained:

$$\left(\frac{d\theta}{dt}\right)^{-1} = \frac{1}{k_a C^b} + t_d = \frac{1}{C^b}\left[\frac{1}{k_a} + \frac{\delta\Gamma^S}{D}\right] \quad (7)$$

According to eq 7, a plot of $(d\theta/dt)^{-1}$ versus $1/C^b$ is linear with an intercept of zero and the slope of this plot can be used, in conjunction with our estimate of $D/\delta\Gamma^S$ ($= 1.7 \pm 0.2 \times 10^7\ cm^3\ mol^{-1}\ s^{-1}$ shown in Figure 9b), to determine k_a. Consistent with this expectation, the corresponding plot for our experimental data (Figure 9d) is linear with an intercept on the $(d\theta/dt)^{-1}$ axis near zero. The value of k_a obtained from this analysis is $(1.9 \pm 0.1) \times 10^4\ M^{-1}\ s^{-1}$, a value somewhat smaller than the k_a values measured for phage−antibody binding in prior work.[30] The "off rate" for the antibody binding, k_d, is much more difficult to estimate because the rate of mass loss of the "loaded" CVS was too slow to accurately measure, but an upper limit of $10^{-5}\ s^{-1}$ can be established based on the absence of measurable mass loss in the 2000 s after each injection (Supporting Information Figure S3). This k_d is slower than is commonly seen for antibody−antigen interactions,[31] and we attribute the low value to the avidity effects from having many bivalent antibodies binding to multivalent phage epitopes within the three-dimensional phage layer coupled with a significant probability of antibody rebinding within this layer. Thus, an upper limit for K_D is $10^{-5}/1.9 \times 10^4\ (s^{-1}/M^{-1}\ s^{-1}) \approx 0.5$ nM. With the use of this K_D value, the validity of the assumption taken with respect to eq 5, that $\theta_{eq} \approx 1.0$, can now be evaluated: at the lowest p-Ab concentration employed here (6.6 nM), $\theta_{eq} = 0.93$, so the error incurred in our estimate of $D/\delta\Gamma^S$ is at most 7%.

Although direct measurements of Γ^S were obtained from the mass measured after exposure of the CVS to single 180 μL injections of 200 nM p-Ab and the desorption of weakly bound p-Ab (Figure 9a), a second estimate of Γ^S was obtained by repeatedly injecting lower concentrations of p-Ab without washing (Figure 10a), and a similar saturation coverage value was obtained. From the average saturation mass increase seen in these two types of experiments ($\approx 3.8 \pm 0.4\ \mu g\ cm^{-2}$), the total number of binding sites can be determined and compared with the phage coverage obtained by the experiment shown in Figure 4. These measured parameters are collected and compared with calculated values in Table 1. From this analysis, we conclude that each M13 virion in the CVS is capable of binding approximately 140 p-Ab molecules. This effective site concentration is lower than the number of P8 peptides on the surface of each phage ($\approx$2700) indicating that many epitopes on the phage surface are unavailable. Two factors that diminish the effective site concentration are[30] (1) physical obstruction of the phage surface by contacts to the SAM and/or proximal phage particles within the immobilized layer and (2) steric crowding of the accessible phage surfaces by bound p-Ab.

Energy dissipation by the QCM sensor surface can also be monitored to gain insight into the nature of the p-Ab/M13 virion interaction. The "motional resistance", R_m, is related to the shear modulus of the surface layer: an increase in the ΔR_m with increasing mass loading is caused by decreases in the shear modulus (mechanical softening) of the surface layer, whereas decreases in ΔR_m indicate an increase in the shear modulus (mechanical stiffening), e.g., refs 32−35. The dissipation factor, D, plays the role of R_m in QCM-D (QCM with dissipation monitoring) measurements.[34,36] Shown in Figure 11a is a plot of R_m versus time for the same experiment shown in Figure 8a. The ΔR_m versus Δf for these data maps onto a single curved plot (Figure 11b), as shown for five of the injections coded in color in Figure 11a (bottom). Both stiffening[37−40] ($\Delta R_m/\Delta f < 0$) and

(30) Katakura, Y.; Zhuang, G. Q.; Nakatani, T.; Furuta, T.; Omasa, T.; Kishimoto, M.; Suga, K.; Shioya, S. *J. Mol. Catal. B: Enzym.* **2004**, *28*, 191−200.

(31) Foote, J.; Eisen, H. N. *Proc. Natl. Acad. Sci. U.S.A.* **1995**, *92*, 1254−1256.

(32) Hook, F.; Rodahl, M.; Brzezinski, P.; Kasemo, B. *Langmuir* **1998**, *14*, 729−734.

(33) Martin, S. J.; Spates, J. J.; Wessendorf, K. O.; Schneider, T. W.; Huber, R. J. *Anal. Chem.* **1997**, *69*, 2050−2054.

(34) Rodahl, M.; Hook, F.; Fredriksson, C.; Keller, C. A.; Krozer, A.; Brzezinski, P.; Voinova, M.; Kasemo, B. *Faraday Discuss.* **1997**, 229−246.

(35) Zilberman, G.; Smith, A. L. *Analyst* **2005**, *130*, 1483−1489.

(36) Rodahl, M.; Hook, F.; Krozer, A.; Brzezinski, P.; Kasemo, B. *Rev. Sci. Instrum.* **1995**, *66*, 3924−3930.

(37) Cavic, B. A.; Chu, F. L.; Furtado, L. M.; Ghafouri, S.; Hayward, G. L.; Mack, D. P.; McGovern, M. E.; Su, H.; Thompson, M. *Faraday Discuss.* **1997**, 159−176.

(38) Gautier, C.; Cougnon, C.; Pilard, J. F.; Casse, N. *J. Electroanal. Chem.* **2006**, *587*, 276−283.

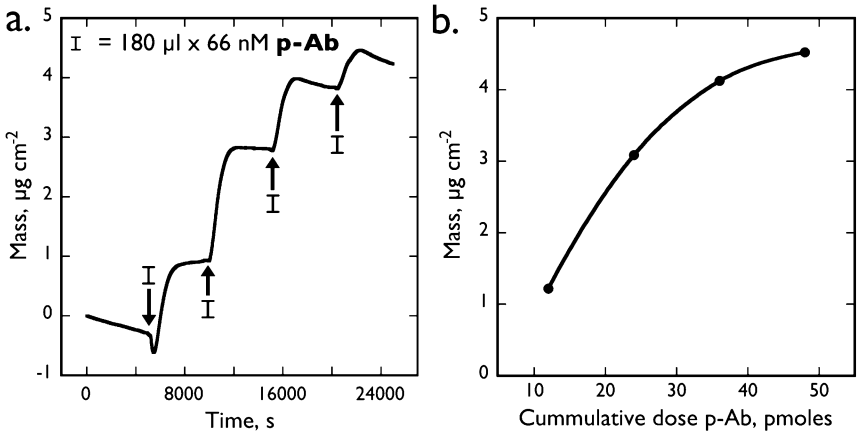

Figure 10. Saturation of p-Ab binding by CVS. (a) Mass vs time trace obtained for four consecutive injections of p-Ab without washing showing the saturation of surface coverage. A flow rate of 10 μL min^{-1} was employed. (b) Plot of accumulated mass, sampled 4000−6000 s after each injection (and just prior to the next injection), vs the number of p-Ab injections.

Table 1. Measured and Calculated or Literature Parameters for the CVS

parameter	calculated or literature value	measured value
phage coverage[a]	0.45 μg cm^{-2} 1.7 × 10^{10} particles cm^{-2}	3.0 ± 0.6 μg cm^{-2} (1.1 ± 0.2) × 10^{11} particles cm^{-2} (≈6.5 phage monolayers)
saturation p-Ab coverage[b]	11.5 μg cm^{-2} 4.6 × 10^{13} molecules cm^{-2}	3.8 ± 0.4 μg cm^{-2} (1.5 ± 0.2) × 10^{13} molecules cm^{-2}
binding sites/ phage particle[c]	2700	140 ± 14
k_a[d]		(1.9 ± 0.1) × 10^{4} M^{-1} s^{-1}
est. k_d[e]		<10^{-5} s^{-1}

[a] The calculated phage coverage assumes crystalline packing of rectangles with dimensions of 1.0 μm in length and 6 nm in diameter, equal to the width and diameter of the M13 virion. The measured coverage was estimated from the mass lost from the CVS after the desorption by UV irradiation, of the virus + SAM layer, as described herein. This total measured mass loss (4.5 ± 0.6 μg cm^{-2}) was reduced by the known, average mass of noncovalently bound phage = 1.5 μg cm^{-2}, which is based upon the irreversible loss of mass seen in the first washing of the CVS using 0.5 M HCl. The mass of a single M13 phage particle is estimated as 16.3 MDa. [b] The calculated saturation coverage is obtained by multiplying the number of phage by the 2700 copies of the P8 peptide present on the surface of each phage particle. The measured saturation coverage was obtained by repetitively injecting p-Ab until mass saturation was observed, as shown in Figure 10. The mass of a single p-Ab molecule, based upon its 148.2 kDa molecular weight, was taken to be 2.46 × 10^{-19} g. [c] The measured value was obtained by dividing the number of phage present by the saturation coverage of p-Ab, assuming that surface and all underlying layers have the same number of active binding sites per unit area. In principle, each phage particle is capable of binding 2700 p-Ab molecules, one at each P8 coat peptide. Though the length of the phage and thus number of P8 epitopes varies in proportion to the quantity of DNA incorporated, our AFM images (e.g., Figure 3a) demonstrate that the phage used here are within the expected length range. [d] k_a calculated from the slope of the plot shown in Figure 9d using eq 5 and a value for $D/\delta\Gamma^S$ of 1.7 × 10^{7} cm^3/mol s. [e] k_d as estimated from mass loss transients recorded for the CVS seen after an exposure to p-Ab (see Supporting Information Figure S3).

softening[32,35,41] ($\Delta R_m/\Delta f > 0$) have been observed previously with increased mass loading for different systems. The CVS layer shows (Figure 11b) increasing R_m indicating that the shear modulus of the CVS is reduced, but the rate of "softening" with increasing mass (i.e., $\Delta R_m/\Delta f$) decreases, resulting in a plot of ΔR_m versus Δf (Figure 11b) that is concave down.

These data can be analyzed in two ways: The total Δf associated with each injection can be plotted versus the total ΔR_m (the blue plot in Figure 11c). Alternatively, the average slope, m, of ΔR_m versus Δf for each injection (Figure 11b) can be plotted versus the total Δf (the red plot in Figure 11c). Both plots show a discontinuity at $\approx\Delta f = 30$ Hz consistent with an increase in the shear modulus, or mechanical stiffness, of the CVS. No quantitative interpretation of ΔR_m versus Δf data has been advanced in the literature, but qualitatively, an increase in the shear modulus of the film could result from the filling of free volume in the phage multilayer by antibody. The cross-linking action of bidentate antibodies on the phage multilayer might also contribute to an increase in the shear modulus, but we have no direct experimental evidence for such cross-linking.

The total ΔR_m observed for each injection in Figure 11a is plotted versus [p-Ab]$^{1/2}$ in Figure 11d, and a clear linear correlation is observed. Although unreported previously to our knowledge, the following is a rationalization for its observation in this system: R_m is known to be proportional to $(\rho\eta)^{1/2}$ where ρ is the density of an adsorbed layer on the QCM surface and η is its viscosity.[32,36,42] The viscosity of protein (e.g., BSA) solutions increases in direct proportion to the protein concentration over

(39) Notley, S. M.; Eriksson, M.; Wagberg, L. *J. Colloid Interface Sci.* **2005**, *292*, 29−37.
(40) Stengel, G.; Hook, F.; Knoll, W. *Anal. Chem.* **2005**, *77*, 3709−3714.
(41) Marx, K. A.; Zhou, T.; Montrone, A.; McIntosh, D.; Braunhut, S. J. *Anal. Biochem.* **2007**, *361*, 77−92.
(42) Muramatsu, H.; Tamiya, E.; Karube, I. *Anal. Chem.* **1988**, *60*, 2142−2146.

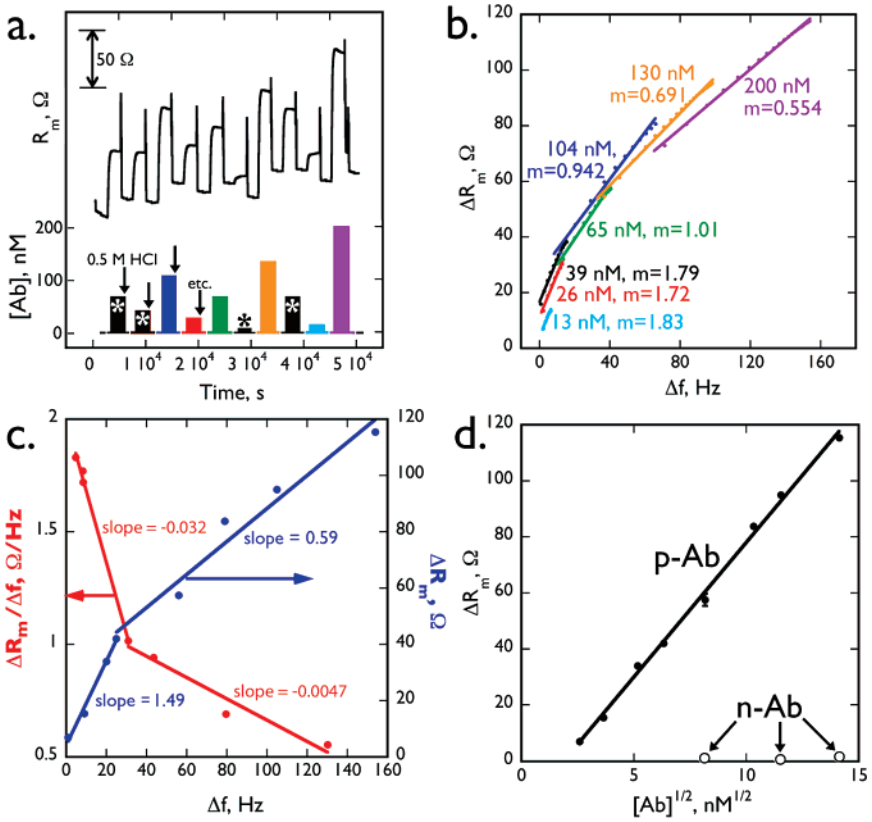

Figure 11. Analysis of the motional resistance, R_m, of the CVS. (a) Plot of the motional resistance, R_m, as a function of time for the same experiment shown in Figure 8a. At bottom is shown the concentration program applied to the surface. A volume of 180 μL of 0.5 M HCl was applied to regenerate the CVS at the times marked with arrows. The color code shown here applies to (b) plot of the motional resistance change, ΔR_m, vs Δf for seven different mass loadings induced by exposure to seven different p-Ab concentrations as indicated (shown in color in (a)). These data map onto a common curve. (c) Two analyses of the data shown in (b). Blue: the maximum change in R_m, $\Delta R_{m,max}$, is plotted vs the maximum change in frequency, Δf_{max}, for each injection. Two quasi-linear regions are observed with slopes of 1.49 Ω Hz^{-1} (low p-Ab concentrations) and 0.981 Ω Hz^{-1} (high p-Ab concentrations), respectively. Red: the slopes of the linear segments plotted in (b) are plotted vs the mean Δf value for each segment. Again, two quasi-linear regions can be discerned with slopes of 0.032 and 0.0047, as shown. (d) Plot of the change of motional resistance, ΔR_m, vs the square root of the p-Ab concentration. Linear regression yields $R^2 = 0.997$ for this plot.

wide ranges in concentration, cf., ref 43, whereas the density of such solutions is very weakly dependent on concentration particularly for dilute solutions.

CONCLUSIONS

The main conclusions of this work are the following:

(1) Attachment of M13 to a gold surface via a SAM of NHS-TE produces a dense (≈6.5 phage monolayers), but porous, covalent virus multilayer. The porosity of this layer is indicated by the ability of each phage particle within it to bind, on average, 140 p-Ab molecules at saturation. This conclusion does not imply that antibody molecules are uniformly distributed across the phage layer. Indeed, it is likely that the number of bound p-Ab is higher near the interface of the phage layer with the solution phase and lower near the gold surface.

(2) A strong and selective affinity of the free M13 phage for the antibody, p-Ab, is retained upon covalent immobilization. No binding of a negative control antibody was detected in this study. The measured k_a of $(1.9 \pm 0.1) \times 10^4$ M^{-1} s^{-1} is lower than the values seen for antibody bonding to free M13 but in the range of the on rates observed for antibody−antigen binding.[31] The measured LOD was 6.6 nM.

(3) The covalent virus layer survives protracted exposure to high ionic strength PBF buffer for periods of 14 h or more. The uptake of p-Ab by the CVS is proportional to p-Ab concentration from 6.6 to 200 nM over this extended period.

(4) Bound antibody is quantitatively removed by exposure of the CVS to 0.5 M HCl with 0.1% Tween 20 enabling the construction of QCM mass versus concentration calibration plots for this surface. The first exposure of the surface to 0.5 M HCl causes the loss of loosely bound phage, but the mass stability of the surface is then retained for multiple acid washings over many hours in flowing wash buffer. An LOD of 6.6 nM and linear mass response (sensitivity = 0.018 μg cm^{-2}/nM) at concentrations from this LOD up to 200 nM was observed for p-Ab binding to the CVS.

(5) As p-Ab is bound to the CVS, we observe a progressive mechanical stiffening at 0.5 μg cm^{-2} of p-Ab, as evidenced, for example, by an inflection in the slope of the ΔR_m versus Δf plot (Figure 11c). An increase in the shear modulus of the film could result from the filling of free volume in the phage multilayer by antibody. Stiffening of the phage layer may be augmented by the

(43) Placidi, M.; Cannistraro, S. *Europhys. Lett.* **1998**, *43*, 476−481.

cross-linking action of bidentate antibodies on an initially floppyand gel-like phage multilayer, but we have no direct experimental evidence for these cross-links.

ACKNOWLEDGMENT

The authors thank Professor Rob Corn for many illuminating discussions and Dr. John Greaves and Professor Paul Gershon for expert assistance with the mass spectrometry of p-Ab. We also thank a reviewer of this manuscript for detailed, constructive comments. R.M.P. acknowledges funding support from the National Science Foundation (Grants CHE-0641169 and DMR-0404057). G.A.W. acknowledges funding support from the NSF (Grant No. EF-0404057).

SUPPORTING INFORMATION AVAILABLE

Additional information as noted in text. This material is available free of charge via the Internet at http://pubs.acs.org.

Received for review July 11, 2007. Accepted November 3, 2007.

AC071470F